

Effective one-dimensional dynamics of elongated Bose-Einstein condensates

A. Muñoz Mateo* and V. Delgado†

Departamento de Física Fundamental II, Universidad de La Laguna, La Laguna, Tenerife, Spain

(Dated: 22 June 2008)

By using a variational approach in combination with the adiabatic approximation we derive a new effective 1D equation of motion for the axial dynamics of elongated condensates. For condensates with vorticity $|q| = 0$ or 1 , this equation coincides with our previous proposal [A. Muñoz Mateo and V. Delgado, Phys. Rev. A **77**, 013617 (2008)]. We also rederive the nonpolynomial Schrödinger equation (NPSE) in terms of the adiabatic approximation. This provides a unified treatment for obtaining the different effective equations and allows appreciating clearly the differences and similarities between the various proposals. We also obtain an expression for the axial healing length of cigar-shaped condensates and show that, in the local density approximation and in units of the axial oscillator length, it coincides with the inverse of the condensate axial half-length. From this result it immediately follows the necessary condition for the validity of the local density approximation. Finally, we obtain analytical formulas that give the frequency of the axial breathing mode with accuracy better than 1%. These formulas can be relevant from an experimental point of view since they can be expressed in terms only of the axial half-length and remain valid in the crossover between the Thomas-Fermi and the quasi-1D mean-field regimes. We have corroborated the validity of our results by numerically solving the full 3D Gross-Pitaevskii equation.

PACS numbers: 03.75.Kk, 05.30.Jp

I. INTRODUCTION

In recent years there has been great interest in the physics of Bose-Einstein condensates of dilute atomic gases confined in highly elongated traps [1, 2, 3, 4, 5, 6, 7, 8, 9]. These systems are routinely produced experimentally by using microfabricated atom chips [10, 11, 12] or tight optical lattices [13, 14] and have important applications in generation and manipulation of matter-wave solitons [15, 16] and in the design of highly sensitive quantum devices such as matter-wave interferometers [17, 18, 19]. From a theoretical point of view, in the mean-field regime and zero temperature limit, they are accurately described in terms of a macroscopic wave function $\psi(\mathbf{r}, t)$ that satisfies the Gross-Pitaevskii equation (GPE) [20]

$$i\hbar \frac{\partial \psi}{\partial t} = \left(-\frac{\hbar^2}{2m} \nabla^2 + V(\mathbf{r}) + gN |\psi|^2 \right) \psi, \quad (1)$$

where N is the number of atoms, $g = 4\pi\hbar^2 a/m$ is the interaction strength determined by the s -wave scattering length a , and $V(\mathbf{r})$ is the potential of the confining trap. In this work we shall restrict ourselves to condensates with repulsive interatomic interactions ($a > 0$).

In highly anisotropic cigar-shaped traps the radial confinement can be so tight that the transversal motion becomes practically reduced to zero-point oscillations. Under these circumstances, only the slow axial degrees of freedom are relevant and the condensate dynamics becomes effectively one-dimensional. This is the quasi-1D mean-field regime. More generally, a high anisotropy always induces two very different time scales. When the axial motion is sufficiently slow in space and time that the radial degrees of freedom can adjust practically instantaneously to the different axial configurations, the radial motion becomes irrelevant and one can still study the condensate dynamics

in terms of an effective equation of lower dimensionality. Several proposals have been made in recent years in this respect [21, 22, 23, 24, 25, 26].

By using the adiabatic approximation and the local chemical potential that follows from a suitable ansatz for the condensate local density [27], we derived in Ref. [28] an effective 1D equation of motion for the axial dynamics of cigar-shaped condensates with repulsive interatomic interactions. We demonstrated that this equation, which is also applicable to condensates containing an axisymmetric vortex of topological charge q , is more accurate than previous proposals. It also has the advantage that it allows to obtain very accurate analytical expressions for a number of ground-state properties, and these expressions remain valid for condensates with an arbitrary number of particles. Despite these merits, from a fundamental point of view it would be desirable to find a more systematic way of deriving this equation. In this work, by using a variational approach in combination with the adiabatic approximation we derive a new effective equation of motion which, for $|q| = 0$ and 1 , coincides exactly with our previous proposal. We also rederive the nonpolynomial Schrödinger equation (NPSE) in terms of the adiabatic approximation. This provides a unified method for obtaining the different effective equations and allows appreciating clearly the differences and similarities between the various proposals. Interestingly, it also demonstrates that in certain cases a variational approach based on the chemical-potential functional can produce more simple and accurate results than the usual variational approach based on the energy functional. We also obtain an expression for the *axial healing length* of cigar-shaped condensates and show that, in the local density approximation and in units of the axial oscillator length, it coincides with the inverse of the ax-

ial half-length. From this result it immediately follows the necessary condition for the validity of the local density approximation. Finally, we obtain analytic formulas that give the frequency of the axial breathing mode of an elongated condensate with accuracy better than 1% and remain valid in the crossover between the Thomas-Fermi (TF) and the quasi-1D mean-field regimes.

II. EFFECTIVE 1D EQUATION OF MOTION

In Ref. [28] we demonstrated that under usual conditions the axial dynamics of highly elongated mean-field condensates with repulsive interatomic interactions, confined in the radial direction by a harmonic potential and containing, in general, an axisymmetric vortex of charge q , can be described by the effective 1D equation

$$i\hbar \frac{\partial \phi}{\partial t} = -\frac{\hbar^2}{2m} \frac{\partial^2 \phi}{\partial z^2} + V_z(z)\phi + \hbar\omega_{\perp} \sqrt{\beta_q^2 + 4aN} |\phi|^2 \phi. \quad (2)$$

This equation incorporates properly the contribution from the transverse degrees of freedom through the term proportional to $\hbar\omega_{\perp}$. The contribution from the vortex is contained entirely in the parameter

$$\beta_q = \frac{2^{2|q|} (|q|!)^2}{(2|q|)!}. \quad (3)$$

The absence of vortices is a particular case corresponding to $q = 0$ and $\beta_q = 1$. Since vortices with $q \geq 2$ are dynamically unstable [29, 30, 31, 32], for condensates containing a multiply quantized vortex the equation above is only applicable up to times shorter than the vortex decay time.

Equation (2) was derived in Ref. [28] by applying the *adiabatic approximation* and using for the corresponding local chemical potential the analytical expression

$$\mu_{\perp}(n_1) = \hbar\omega_{\perp} (|q| + 1 - \beta_q) + \hbar\omega_{\perp} \sqrt{\beta_q^2 + 4an_1}. \quad (4)$$

This expression, in turn, follows from an approximation scheme based on a suited TF-like ansatz for the condensate local density which, essentially, represents a simple extension of the Thomas-Fermi approximation [27]. In what follows we will give an alternative derivation that permits obtaining the above result in a more systematic way. To this end, it is convenient to recall very briefly the main steps that led us to Eq. (2). Under usual conditions, the time scales characterizing the axial and the radial dynamics of highly elongated condensates are so different that one can appeal to the adiabatic approximation and factorize the condensate wave function as [21, 33]

$$\psi(\mathbf{r}, t) = \varphi(\mathbf{r}_{\perp}; n_1(z, t)) \phi(z, t), \quad (5)$$

where $\mathbf{r}_{\perp} = (x, y)$ and $n_1(z, t)$ is the local density per unit length along z

$$n_1(z, t) \equiv N \int d^2\mathbf{r}_{\perp} |\psi(\mathbf{r}_{\perp}, z, t)|^2 = N |\phi(z, t)|^2. \quad (6)$$

Substituting Eq. (5) into the GPE and assuming that the axial density varies sufficiently slowly in space and time, one obtains [28]

$$i\hbar \frac{\partial \phi}{\partial t} = -\frac{\hbar^2}{2m} \frac{\partial^2 \phi}{\partial z^2} + V_z(z)\phi + \mu_{\perp}(n_1)\phi, \quad (7)$$

$$\left(-\frac{\hbar^2}{2m} \nabla_{\perp}^2 + V_{\perp}(\mathbf{r}_{\perp}) + gn_1 |\varphi|^2 \right) \varphi = \mu_{\perp}(n_1)\varphi, \quad (8)$$

where we also have assumed a separable confining potential $V(\mathbf{r}) = V_{\perp}(\mathbf{r}_{\perp}) + V_z(z)$. Equation (7) shows that the axial dynamics is affected by the radial degrees of freedom only via the transverse local chemical potential $\mu_{\perp}(n_1)$. Equation (8), which is a *stationary* GPE, reveals that, at every instant t , the transverse wave function φ coincides locally with the equilibrium wave function of an axially uniform condensate characterized by a linear density $n_1(z, t)$. This result simply reflects the fact that, for highly elongated condensates, at every instant of time the (fast) transverse degrees of freedom can adjust instantaneously to the local equilibrium configuration compatible with the axial configuration of the condensate.

In what follows, we shall consider the confining potential to be axisymmetric and harmonic in the radial direction, while it remains generic in the axial direction

$$V(\mathbf{r}) = \frac{1}{2}m\omega_{\perp}^2 r_{\perp}^2 + V_z(z). \quad (9)$$

Using that $\mu_{\perp}(n_1)$ as given by Eq. (4) is an accurate approximate solution of Eq. (8), after substituting in Eq. (7) and taking into account Eq. (6), one finally arrives at Eq. (2).

Other different effective equations of motion can be obtained by using the adiabatic approximation in combination with a variational approach. To see this, it is convenient to consider the axially uniform condensate described by the transverse equation (8) as composed of an infinite series of identical pieces of length L , with periodic boundary conditions, and containing N particles each. The exact solutions of this equation are the critical points of the energy functional

$$\frac{E[\varphi]}{N} \equiv \int d^2\mathbf{r}_{\perp} \left(\frac{\hbar^2}{2m} |\nabla_{\perp} \varphi|^2 + V_{\perp} |\varphi|^2 + \frac{1}{2}gn_1 |\varphi|^4 \right), \quad (10)$$

where $n_1 = N/L$ is the density per unit length. Thus, the problem of finding the eigenfunctions φ that satisfy Eq. (8) is equivalent to the problem of finding, within the *whole* space of admissible functions, those functions that make the above energy functional stationary. The corresponding local chemical potential then follows from the relationship:

$$\mu_{\perp}(n_1) = \frac{\partial E[\varphi]}{\partial N}. \quad (11)$$

In general, however, both problems are equally complicated, so that, in practice, one usually has to limit the search

for the critical points of $E[\varphi]$ to a subspace of convenient variational trial functions. The solutions so obtained, in general, no longer satisfy exactly the transverse equation (8), and the corresponding energy $E[\varphi]$ and chemical potential $\mu_{\perp}(n_1)$ can only be considered as mere estimations of the actual values.

Multiplying by φ^* and integrating on the radial coordinates, Eq. (8) leads to the chemical-potential functional

$$\mu_{\perp}[\varphi] \equiv \int d^2 \mathbf{r}_{\perp} \varphi^* \left(-\frac{\hbar^2}{2m} \nabla_{\perp}^2 + V_{\perp}(\mathbf{r}_{\perp}) + gn_1 |\varphi|^2 \right) \varphi. \quad (12)$$

Since for condensates with repulsive interatomic interactions $\mu_{\perp}[\varphi]$ is bounded from below, an independent estimation for the local chemical potential of the ground state can be obtained by minimizing directly the above functional. In the ideal-gas perturbative regime ($g \rightarrow 0$) the system becomes quasi-linear and both estimates coincide. In general, however, Eqs. (10) and (12) lead to different results. When the search is performed within the whole space of admissible functions, minimization of the energy functional always yields the correct result. However, as we shall see, when the search is restricted to a subspace of variational trial functions (as is usually the case), the direct minimization of the functional (12) can lead to a better result for the chemical potential of the ground state.

To the lowest order in the perturbative regime, the ground-state solution of Eq. (8) compatible with an axisymmetric vortex of charge q takes the form [27]

$$\varphi_q(r_{\perp}, \theta) = \frac{\exp(iq\theta)}{\sqrt{\pi a_{\perp}^2 |q|!}} (r_{\perp}/a_{\perp})^{|q|} \exp(-r_{\perp}^2/2a_{\perp}^2), \quad (13)$$

where $a_{\perp} = \sqrt{\hbar/m\omega_{\perp}}$ is the oscillator length. It is then natural to look for the critical points of the energy functional (10) within the subspace composed of the above functions with the substitution $a_{\perp} \rightarrow \Gamma a_{\perp}$, where Γ is a dimensionless variational parameter determining the condensate width [34, 35]. Minimization of Eq. (10) thus yields

$$\Gamma = \left(1 + \frac{2an_1}{(|q|+1)\beta_q} \right)^{1/4}. \quad (14)$$

Substituting in Eq. (10) one obtains the condensate energy

$$\frac{E}{N} = \hbar\omega_{\perp}(|q|+1) \sqrt{1 + \frac{2an_1}{(|q|+1)\beta_q}}. \quad (15)$$

Using this expression in Eq. (11) one finally finds the desired chemical potential

$$\mu_{\perp} = \hbar\omega_{\perp}(|q|+1) \frac{1 + \frac{3an_1}{(|q|+1)\beta_q}}{\sqrt{1 + \frac{2an_1}{(|q|+1)\beta_q}}}. \quad (16)$$

Substitution of Eq. (16) into Eq. (7) then leads to the following effective 1D equation, to be compared to Eq. (2):

$$i\hbar \frac{\partial \phi}{\partial t} = -\frac{\hbar^2}{2m} \frac{\partial^2 \phi}{\partial z^2} + V_z(z)\phi + \hbar\omega_{\perp}(|q|+1) \frac{1 + \frac{3aN|\phi|^2}{(|q|+1)\beta_q}}{\sqrt{1 + \frac{2aN|\phi|^2}{(|q|+1)\beta_q}}}. \quad (17)$$

This equation, derived here by using the standard adiabatic approximation, is nothing but the nonpolynomial Schrödinger equation (NPSE) [36]. Equation (17) is also applicable to condensates with attractive interatomic interactions.

As already said, one can still obtain a different effective equation of motion by estimating the chemical potential directly from the functional (12). In doing so, one finds a condensate width

$$\Gamma = \left(1 + \frac{4an_1}{(|q|+1)\beta_q} \right)^{1/4}, \quad (18)$$

and, after substitution in Eq. (12) one arrives at the following expression for the local chemical potential:

$$\mu_{\perp} = \hbar\omega_{\perp}(|q|+1) \sqrt{1 + \frac{4an_1}{(|q|+1)\beta_q}}. \quad (19)$$

Substituting again in Eq. (7) one finally obtains

$$i\hbar \frac{\partial \phi}{\partial t} = -\frac{\hbar^2}{2m} \frac{\partial^2 \phi}{\partial z^2} + V_z(z)\phi + \hbar\omega_{\perp}(|q|+1) \sqrt{1 + \frac{4aN|\phi|^2}{(|q|+1)\beta_q}}. \quad (20)$$

This equation, to be compared to Eqs. (2) and (17), is a new effective 1D equation governing the axial dynamics of the condensate. As can be easily verified, for $|q| = 0$ and 1 the equation above coincides exactly with our previous proposal (2). This is remarkable since the chemical potentials that lead to both equations have been derived by applying very different techniques: while the chemical potential (19) follows from a variational approach, the chemical potential (4) was derived in Ref. [27] by using a suited TF-like ansatz for the condensate local density. This non-trivial coincidence provides additional support to our previous results. Note also that, from a dynamical point of view, these cases (corresponding to $|q| = 0$ and 1) are precisely the most relevant ones, since for condensates with a larger vortex charge the applicability of the above equations is limited to times shorter than the vortex lifetime. For $|q| \geq 2$, Eqs. (2) and (20) give somewhat different results, which is a consequence of the different way in which the chemical potentials (4) and (19) incorporate the effect of the vortex. The point is to determine which of the above equations give better results. In Ref. [28] we demonstrated that, for $q = 0$, Eq. (2) is somewhat more accurate than Eq.

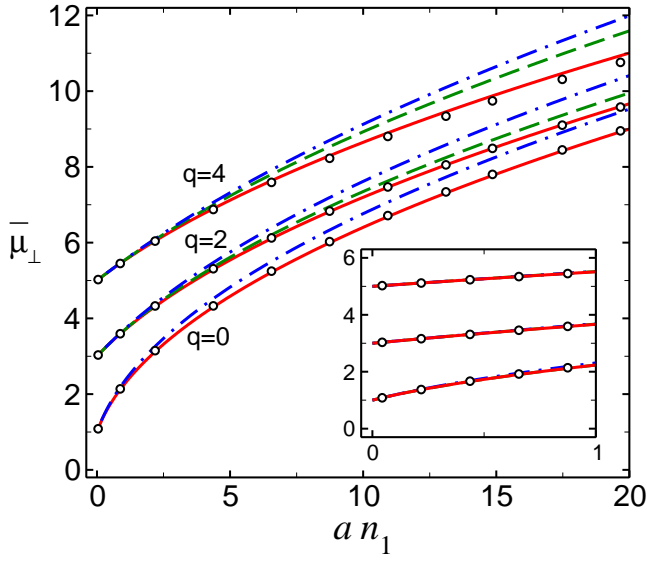


FIG. 1: Different theoretical estimates for the local chemical potential $\bar{\mu}_\perp = \mu_\perp/\hbar\omega_\perp$ as a function of an_1 . Solid lines have been obtained from Eq. (4), dashed lines from Eq. (19), and dash-dotted lines from Eq. (16). Open circles are exact results obtained by solving numerically Eq.(8) with no approximations.

(17). It remains to be seen whether this is also the case for condensates containing a vortex. It is clear that the ability of the above equations for reproducing accurately the axial dynamics of the condensate is directly related to the ability of the corresponding chemical potentials (4), (16), and (19) for reproducing accurately the lowest eigenvalue of the transverse equation (8).

Figure 1 compares the different theoretical estimates for the local chemical potential, obtained from the above formulas, with exact results (open circles) obtained by solving numerically Eq. (8), with no approximations, for a wave function of the form $\exp(iq\theta)\varphi(r_\perp)$ with $q = 0, 2$ and 4 . As seen in Ref. [28] our chemical potential, Eq. (4), (solid lines) is in good agreement with the numerical results. The maximum error is smaller than 1% for $q = 0$ and 2 , and smaller than 2.5% for $q = 4$, and this is so for any value of the dimensionless interaction parameter an_1 (not only in the range shown in the figure). As mentioned before, the theoretical estimate from Eq. (19) (dashed lines) coincides exactly with that from Eq. (4) for $q = 0$ (and also for $q = 1$, not shown in the figure). For $q = 2$ the maximum error (in the range of the figure) is of the order of 3% and for $q = 4$ it is of the order of 7%. The estimate from Eq. (16) (dash-dotted lines) turns out to be somewhat less accurate. In this case the maximum error is of the order of 5% for $q = 0$, of the order of 7% for $q = 2$, and of the order of 10% for $q = 4$. Moreover, these errors continue increasing with an_1 . These results indicate that the effective 1D equation (2) should give a better description of the condensate dynamics than the two other alternative equations.

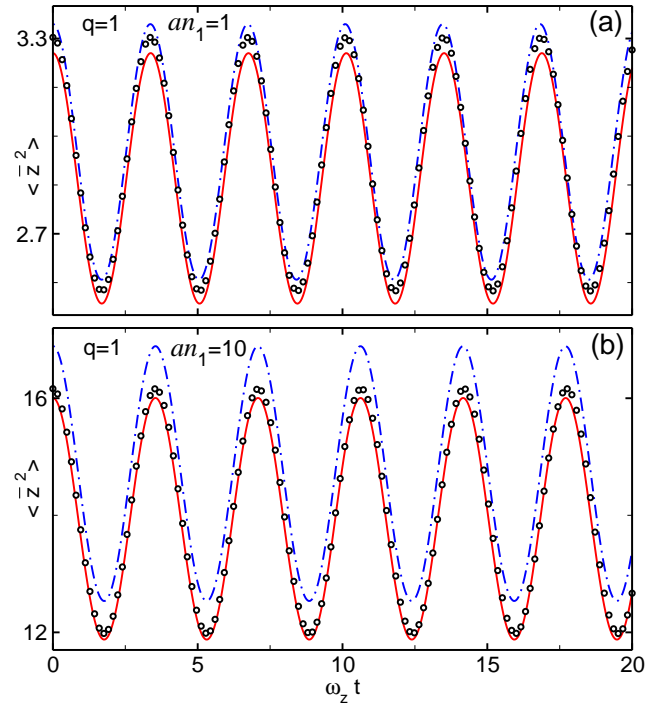


FIG. 2: Evolution of $\langle z^2 \rangle$ for an elongated condensate with $q = 1$, after a perturbation that excites its axial breathing mode ($\bar{z} \equiv z/a_z$). Solid lines have been obtained from Eq. (2), dashed lines from Eq. (20), and dash-dotted lines from Eq. (17). Open circles are exact results obtained from the full 3D GPE.

To verify this point we have studied the dynamical evolution of an elongated condensate with $\lambda = 0.1$ after a sudden perturbation that excites its axial breathing mode. Figures 2 and 3 show the evolution in time of the mean squared axial amplitude $\langle z^2 \rangle = N^{-1} \int dz z^2 n_1(z, t)$ after a sudden perturbation at $t = 0$ in the axial confinement frequency of the form $\omega_z \rightarrow 1.1\omega_z$. Figure 2 corresponds to a condensate containing a vortex of charge $q = 1$ while Fig. 3 corresponds to a condensate containing a $q = 3$ vortex. Solid lines have been obtained from our effective equation (2), dashed lines have been obtained from the variational equation (20), and dash-dotted lines from the NPSE (17). Open circles are exact results obtained by solving numerically the full 3D GPE with no approximations. Since all the three effective equations have the correct perturbative ($an_1 \ll 1$) limit (see inset in Fig. 1), they turn out to be practically indistinguishable in this regime. As Fig. 2(a) shows, for condensates with $q = 1$ and a (dimensionless) peak axial density $an_1 = 1$ these equations still give rather similar results. The differences increase as an_1 does, as expected from Fig. 1. This can be appreciated from Fig. 2(b) which corresponds to a condensate with $an_1 = 10$. In this case Eqs. (2) and (20), which for $q = 1$ are indistinguishable, give more accurate results (solid lines) than Eq. (17) (dash-dotted lines).

As Fig. 3(a) shows, for $q = 3$ Eq. (2) gives somewhat

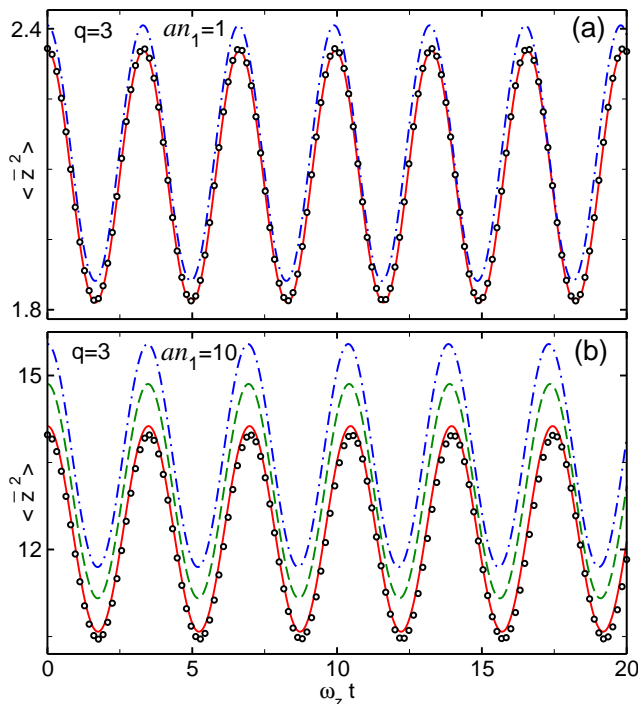


FIG. 3: Evolution of $\langle \bar{z}^2 \rangle$ for an elongated condensate with $q = 3$, after a perturbation that excites its axial breathing mode ($\bar{z} \equiv z/a_z$). Solid lines have been obtained from Eq. (2), dashed lines from Eq. (20), and dash-dotted lines from Eq. (17). Open circles are exact results obtained from the full 3D GPE.

better results than the two other ones even for condensates with a peak axial density $an_1 = 1$. In this case, the results from Eq. (20) (not shown in the figure for clarity) lie exactly in between the two curves shown. Again, as Fig. 3(b) reflects, the differences become more evident as an_1 increases. These results indicate that the effective 1D equation (2) is the one that gives a more accurate description of the condensate dynamics. It is important to note, however, that for condensates with $|q| = 0$ or 1 this equation coincides exactly with the variational equation (20).

Equation (2) has the additional advantage that, in combination with the local density approximation (whose conditions of validity will be analyzed in detail in Section III), it allows to derive a number of useful analytical expressions for the ground-state properties of elongated condensates [28]. We next give those that will be needed later on. Consider a trapping potential that is also harmonic in the axial direction $V_z(z) = \frac{1}{2}m\omega_z^2 z^2$, with $a_z = \sqrt{\hbar/m\omega_z}$ being the axial oscillator length and $\lambda = \omega_z/\omega_\perp$ the trap aspect ratio. Then, it can be shown that the total chemical potential is given by [28]

$$\frac{\mu}{\hbar\omega_\perp} = (|q| + 1) + \frac{1}{2}(\sqrt{\lambda}\bar{Z})^2, \quad (21)$$

where $\bar{Z} = Z/a_z$ is the dimensionless axial half-length. The axial density profile follows from the formula

$$n_1^0(z) = \beta_q \frac{(\sqrt{\lambda}\bar{Z})^2}{4a} \left(1 - \frac{z^2}{Z^2}\right) + \frac{(\sqrt{\lambda}\bar{Z})^4}{16a} \left(1 - \frac{z^2}{Z^2}\right)^2 \quad (22)$$

with $n_1^0(z) = 0$ for $|z| > Z$. The interest of the above formulas lies in the fact that they are valid and accurate (with an accuracy typically better than 1%) not only in the TF and in the quasi-1D mean-field regime, but also in between these two limiting cases. Moreover, since they only depend on an easily measurable physical quantity (the condensate axial half-length) they can be useful for a more precise experimental characterization of these kind of systems. In the present work we will use these expressions in order to derive an approximate analytical formula for the frequencies of the axial breathing mode of elongated condensates.

It can be shown that the axial half-length satisfies the following polynomial equation [28]:

$$\frac{1}{15}(\sqrt{\lambda}\bar{Z})^5 + \frac{1}{3}\beta_q(\sqrt{\lambda}\bar{Z})^3 = \chi_1, \quad (23)$$

with

$$\chi_1 \equiv \frac{\lambda N a}{a_\perp}. \quad (24)$$

An approximate solution that satisfies the above equation for any $\chi_1 \in [0, \infty)$, with a residual error [27] smaller than 0.75% for $q = 0$ and smaller than 3.2% for $1 \leq |q| \leq 10$ is given by

$$\sqrt{\lambda}\bar{Z} = \left[\frac{1}{(15\chi_1)^{\frac{4}{5}} + \frac{1}{3}} + \frac{1}{57\chi_1 + 345} + \frac{1}{(3\chi_1/\beta_q)^{\frac{4}{3}}} \right]^{-\frac{1}{4}} \quad (25)$$

It is clear that the variational equation (20) also permits deriving analytical expressions for the relevant ground-state properties. For $|q| = 0$ and 1 one obtains the same expressions (21)–(25). For $|q| \geq 2$, the only modification is that the second term on the right-hand side of Eq. (22) and the first term on the left-hand side of Eq. (23) become multiplied by the factor $\beta_q/(|q| + 1)$. As expected from Fig. 1, these modified equations turn out to be somewhat less accurate than the above equations, and for this reason, except for the present Section, we shall not consider them further in this work. Substitution of Eqs. (6) and (13) (with $a_\perp \rightarrow \Gamma a_\perp$) into Eq. (5) leads to the equilibrium variational wave function

$$\psi(\mathbf{r}) = \frac{\exp(iq\theta)}{\Gamma a_\perp \sqrt{\pi|q|!}} \left(\frac{r_\perp}{\Gamma a_\perp}\right)^{|q|} \exp\left(-\frac{r_\perp^2}{2\Gamma^2 a_\perp^2}\right) \sqrt{\frac{n_1^0(z)}{N}}, \quad (26)$$

where $\Gamma(n_1^0)$ is the (z -dependent) equilibrium condensate width given by Eq. (18) and $n_1^0(z)$ is the axial density profile given by Eq. (22) (conveniently modified if $|q| \geq 2$). On the other hand, from the equilibrium condensate density $n(\mathbf{r}) = N|\psi(\mathbf{r})|^2$ one finds the following expression

relating the peak density $n(\mathbf{0})$ with the peak axial density $n_1^0(0)$ of a cigar-shaped condensate with no vortices:

$$n(\mathbf{0}) = \frac{n_1^0(0)}{\pi a_\perp^2 \sqrt{1 + 4an_1^0(0)}}. \quad (27)$$

Since $an_1^0(0) = (\sqrt{\lambda} \bar{Z}/2)^2 + (\sqrt{\lambda} \bar{Z}/2)^4$, the above formula can also be used to obtain $n(\mathbf{0})$ as a function of Z . Equation (27) has the correct limits in the two extreme regimes. In particular, in the perturbative regime ($an_1 \ll 1$) it reduces to $n(\mathbf{0}) = n_1^0(0)/\pi a_\perp^2$, whereas in the TF regime ($an_1 \gg 1$) it takes the form $n(\mathbf{0}) = \sqrt{n_1^0(0)/a}/2\pi a_\perp^2$.

III. AXIAL HEALING LENGTH

For later purposes, it is convenient to rewrite the effective 1D equation (2) in terms of an equivalent system of hydrodynamic equations describing the superfluid dynamics of the condensate [37]. To this end we write the axial wave function in polar form

$$\sqrt{N}\phi(z, t) = \sqrt{n_1(z, t)}e^{iS(z, t)}. \quad (28)$$

By substituting in Eq. (2), one arrives after some algebra at the following equations governing the evolution in time of the axial density n_1 and velocity field $v \equiv (\hbar/m)\partial S/\partial z$:

$$\frac{\partial n_1}{\partial t} + \frac{\partial}{\partial z}(n_1 v) = 0, \quad (29)$$

$$m \frac{\partial v}{\partial t} + \frac{\partial}{\partial z} \left(\mu_\perp(n_1) + V_z + \frac{1}{2} m v^2 - \frac{\hbar^2}{2m\sqrt{n_1}} \frac{\partial^2}{\partial z^2} \sqrt{n_1} \right) = 0. \quad (30)$$

In these equations, that are completely equivalent to Eq. (2), the mean-field interaction energy between atoms enters through the local chemical potential $\mu_\perp(n_1)$ given by Eq. (4). The term proportional to \hbar^2 is the quantum pressure, which has its origin in the quantum kinetic energy of the system. Note that $\mu_\perp(n_1)$ can always be written as

$$\mu_\perp(n_1) = \hbar\omega_\perp(|q| + 1) + \tilde{\mu}_\perp(n_1). \quad (31)$$

This can be seen from the transverse equation (8), whose exact perturbative solution is an infinite series of the form $\mu_\perp(n_1) = \hbar\omega_\perp(|q| + 1) + 2\beta_q^{-1}\hbar\omega_\perp an_1 + \dots$. From Eq. (30) it is thus clear that the last term on the right-hand side of Eq. (31) is the only one that contributes to the dynamics. Taking this into account, and defining, as usual, the axial healing length ξ_z as the length scale for which the spatial variations in the condensate density induce a quantum pressure comparable in magnitude to the contribution from the interaction energy, i.e.,

$$\frac{\hbar^2}{2m\xi_z^2} \sim \tilde{\mu}_\perp(n_1), \quad (32)$$

one obtains the following expression for the axial healing length of elongated condensates:

$$\xi_z = \frac{\hbar}{\sqrt{2m[\mu_\perp(n_1) - \hbar\omega_\perp(|q| + 1)]}}. \quad (33)$$

In the absence of vortices ($q = 0$), the above formula reduces to that introduced in Ref. [28]. When the length scale Δ_z of the spatial variations of the condensate density along z is much greater than ξ_z the contribution from the quantum pressure becomes negligible in comparison with the contribution from the interaction energy, and Eq. (30) reduces to

$$m \frac{\partial v}{\partial t} + \frac{\partial}{\partial z} \left(\mu_\perp(n_1) + V_z + \frac{1}{2} m v^2 \right) = 0. \quad (34)$$

In the stationary state $v = 0$, and the above equation leads to

$$\mu = \mu_\perp(n_1^0) + V_z(z), \quad (35)$$

where $n_1^0(z)$ denotes the equilibrium density per unit length and μ is the total chemical potential of the condensate. Equation (35), which holds whenever $\Delta_z \gg \xi_z$ and involves no additional approximations, is the so-called local density approximation.

In what follows, we shall consider a stationary condensate confined by a trapping potential that is also harmonic in the axial direction $V_z(z) = \frac{1}{2}m\omega_z^2 z^2$. Substituting Eqs. (35) and (21) into Eq. (33) one finds the following expression for the *local* axial healing length of an elongated condensate in the local density approximation:

$$\frac{\xi_z(z)}{a_z} = \frac{(Z/a_z)^{-1}}{\sqrt{1 - z^2/Z^2}}. \quad (36)$$

This formula shows that at the condensate edges the axial healing length diverges, which is an expected result since in this region the kinetic energy can never be neglected in comparison with the interaction energy. Defining, as is usual, the healing length of the condensate as the healing length at the center of the density cloud one arrives at

$$\frac{\xi_z}{a_z} = \left(\frac{Z}{a_z} \right)^{-1}. \quad (37)$$

This formula reflects that in the local density approximation and in units of the axial oscillator length, the healing length of the condensate coincides with the inverse of its axial half-length. As already said, in order for the local density approximation to be valid it is sufficient that $\xi_z \ll \Delta_z$. Thus, taking into account that for a condensate in its stationary state Δ_z is of the order of Z , it follows from Eq. (37) that the validity of the local density approximation requires the condition

$$\frac{Z}{a_z} \gg \left(\frac{Z}{a_z} \right)^{-1}. \quad (38)$$

It can be easily verified that in the intermediate and TF regimes the condition $\lambda \ll 1$ (which always holds for

elongated condensates) already guarantees the above requirement. In the quasi-1D mean-field regime, however, the trap aspect ratio λ must be sufficiently small so as to satisfy the inequality (38). Taking into account that in this regime $an_1^0(0) \simeq \beta_q(\sqrt{\lambda} \bar{Z}/2)^2$, one finds that the validity of the local density approximation in the perturbative ($an_1^0 \ll 1$) regime requires the condition

$$\lambda \ll \frac{4an_1^0(0)}{\beta_q}. \quad (39)$$

Alternatively, using that for $\chi_1 \ll 1$ one has $\chi_1 \simeq (\beta_q/3)(\sqrt{\lambda} \bar{Z})^3$, the above condition can also be written as

$$\lambda \ll \left(\frac{3\chi_1}{\beta_q} \right)^{2/3}. \quad (40)$$

IV. COLLECTIVE OSCILLATIONS

We are interested in obtaining an analytic formula for the frequency of the axial breathing mode of elongated condensates, applicable also in the crossover between the TF and the quasi-1D mean-field regimes. To this end we will use the hydrodynamical equation (34). Considering small linear oscillations around the equilibrium configuration $n_1 = n_1^0 + \delta n_1$ and $v = \delta v$, after linearization, Eq. (34) takes the form

$$m \frac{\partial}{\partial t} \delta v + \frac{\partial}{\partial z} \left(\mu_{\perp}(n_1^0) + \left. \frac{\partial \mu_{\perp}}{\partial n_1} \right|_0 \delta n_1 + V_z \right) = 0, \quad (41)$$

Taking into account Eq. (35), the above equation reduces to

$$m \frac{\partial}{\partial t} \delta v + \frac{\partial}{\partial z} \left(\left. \frac{\partial \mu_{\perp}}{\partial n_1} \right|_0 \delta n_1 \right) = 0, \quad (42)$$

where, from Eq. (4), one has

$$\left. \frac{\partial \mu_{\perp}}{\partial n_1} \right|_0 = \frac{2a\hbar\omega_{\perp}}{\sqrt{\beta_q^2 + 4an_1^0}}, \quad (43)$$

with $n_1^0(z)$ given by Eq. (22). We look for solutions of Eq. (42) in the form of (axial) dilatations [38, 39], that is, we introduce a scaling parameter $b(t)$ satisfying the relationships $z = b(t)z_0$ and $v = \dot{b}(t)z_0 = z\dot{b}(t)/b(t)$, and assume that the axial density cloud at any t is related to its initial value as

$$n_1(z, t) = \frac{1}{b(t)} n_1^0(z_0) = \frac{1}{b(t)} n_1^0\left(\frac{z}{b(t)}\right). \quad (44)$$

For linear oscillations, the case we are interested in, $b(t) = 1 + \delta b(t)$ and $\delta v = \delta \dot{b}(t)z$ with $\delta b(t) = \delta b_0 e^{-i\omega t}$. Thus, the first term in Eq. (42) takes the form

$$m \frac{\partial}{\partial t} \delta v = -m\omega^2 z \delta b. \quad (45)$$

As for the second term, we note that taking into account Eq. (44), δn_1 can be written as

$$\delta n_1 = \left. \frac{\partial n_1}{\partial b} \right|_{b=1} \delta b = - \left[\left(1 + z \frac{\partial}{\partial z} \right) n_1^0(z) \right] \delta b. \quad (46)$$

Using now Eq. (22), one finds

$$\delta n_1 = \left[\frac{(\sqrt{\lambda} \bar{Z})^2 z^2}{2a} \left\{ \beta_q + \frac{(\sqrt{\lambda} \bar{Z})^2}{2} \left(1 - \frac{z^2}{Z^2} \right) \right\} - n_1^0 \right] \delta b \quad (47)$$

From Eqs. (4), (35) and (21) one has

$$\sqrt{\beta_q^2 + 4an_1^0} - \beta_q = \frac{(\sqrt{\lambda} \bar{Z})^2}{2} \left(1 - \frac{z^2}{Z^2} \right). \quad (48)$$

Using this relationship in Eq. (47) we obtain

$$\delta n_1 = \left[\frac{(\sqrt{\lambda} \bar{Z})^2 z^2}{2a} \sqrt{\beta_q^2 + 4an_1^0} - n_1^0 \right] \delta b. \quad (49)$$

Substituting now Eqs. (43), (49) and (22) into the second term of Eq. (42), after some algebra one finally obtains

$$\frac{\partial}{\partial z} \left(\left. \frac{\partial \mu_{\perp}}{\partial n_1} \right|_0 \delta n_1 \right) = m\Omega^2(z) \omega_z^2 z \delta b, \quad (50)$$

where

$$\Omega^2(z) \equiv \left(3 - \frac{2an_1^0(z)}{\beta_q^2 + 4an_1^0(z)} \right). \quad (51)$$

From Eqs. (45) and (50) it is then clear that only in the TF and the quasi-1D mean-field regimes Eq. (42) admit solutions in the form of dilatations. In the TF regime one has $4an_1^0 \gg \beta_q^2$ and as a consequence $\Omega^2(z) = 5/2$. In this case, Eq. (42) reflects that the axial breathing mode is an oscillatory dilatation with a frequency $\omega^2 = (5/2)\omega_z^2$, in good agreement with previous results [37]. In the quasi-1D mean-field regime $4an_1^0 \ll \beta_q^2$ and one obtains the well-known result $\omega^2 = 3\omega_z^2$ [40, 41, 42]. In between these two limiting cases, however, the condensate dynamics does not depart too much from a dilatation. This is a direct consequence of the fact that $\Omega^2(z)$ as given by Eq. (51) is a slowly varying function of z that can be well approximated by its mean value

$$\Omega^2(z) \approx \frac{1}{2Z} \int_{-Z}^{+Z} \left(3 - \frac{2an_1^0}{\beta_q^2 + 4an_1^0} \right) dz. \quad (52)$$

Substituting Eq. (22) and performing the integration one obtains the following analytical expression for the frequency of the axial breathing mode of a highly elongated condensate:

$$\frac{\omega^2}{\omega_z^2} = \Omega^2 \approx \frac{5}{2} + \frac{1}{2(\zeta^2 + 2)} + \frac{\tanh^{-1}(\zeta/\sqrt{\zeta^2 + 2})}{\zeta(\zeta^2 + 2)^{3/2}}, \quad (53)$$

where $\zeta \equiv \sqrt{\lambda/\beta_q} \bar{Z}$. It can be easily verified that the above formula has the correct limits in both the TF and the quasi-1D mean-field regimes. According to Eq. (53) one

can obtain ω^2 experimentally from a measurement of the condensate axial half-length Z in the equilibrium configuration. Alternatively one can also use Eq. (25) to express ω^2/ω_z^2 as a function only of χ_1 and β_q .

One can still derive an independent analytic estimate for ω^2 by using the formula [6]

$$\omega^2 = -2 \frac{\langle z^2 \rangle}{d\langle z^2 \rangle/d\omega_z^2}. \quad (54)$$

This formula, which follows from a sum-rule approach, gives an upper bound to the frequency of the axial breathing mode. Substituting Eq. (22) in the mean squared amplitude

$$\langle z^2 \rangle = N^{-1} \int dz z^2 n_1^0(z), \quad (55)$$

and carrying out the integration, Eq. (54) becomes

$$\frac{\omega^2}{\omega_z^2} = \frac{8(\zeta^2 + 7)}{7 - \zeta^2 - (70 + 14\zeta^2)\Sigma}, \quad (56)$$

where $\Sigma = (\lambda/\bar{Z}) d\bar{Z}/d\lambda$. The derivative with respect to λ can be conveniently rewritten as

$$\frac{d\bar{Z}}{d\lambda} = \frac{1}{\lambda\sqrt{\lambda}} \left[\chi_1 \frac{d(\sqrt{\lambda}\bar{Z})}{d\chi_1} - \frac{1}{2}(\sqrt{\lambda}\bar{Z}) \right]. \quad (57)$$

Now the derivative on the right-hand side can be obtained from Eq. (23). In doing so, one finds

$$\Sigma = \frac{\chi_1}{5\chi_1 - \frac{2}{3}\beta_q(\sqrt{\lambda}\bar{Z})^3} - \frac{1}{2}. \quad (58)$$

Substituting this result in Eq. (56) and using again Eq. (23) to eliminate ζ^5 in favor of ζ^3 one finally obtains

$$\frac{\omega^2}{\omega_z^2} = \frac{4\beta_q^{5/2}\zeta^3 - 15\chi_1(\zeta^2 + 5)}{3\beta_q^{5/2}\zeta^3 - 6\chi_1(\zeta^2 + 5)}, \quad (59)$$

where $\zeta \equiv \sqrt{\lambda/\beta_q}\bar{Z}$. As before, taking into account that according to Eq. (23) χ_1 can be rewritten in terms of Z , the above equation shows that ω^2 can be obtained experimentally from a measurement of the axial half-length in the equilibrium configuration. By using Eq. (25) one can also rewrite ω^2/ω_z^2 as a function only of χ_1 and β_q . Equations (53) and Eq. (59) have been obtained under the assumption that the quantum pressure has a negligible contribution. This implies that in the quasi-1D mean-field regime ($\chi_1 \ll 1$) the trap aspect ratio λ must be sufficiently small so as to satisfy the requirement (40). In the intermediate and TF regimes, however, the condition $\lambda \ll 1$ already guarantees the inequality (38) to hold true. It can be easily verified that Eqs. (53) and (59) coincide each other within 0.65% for $q = 0$ and within 0.77% for $q = 1$. In order to determine to what extent the above formulas reproduce the experimental results we have performed a computer experiment based on the numerical solution of the full 3D Gross-Pitaevskii equation (1). We have considered ^{87}Rb condensates at zero temperature confined in a

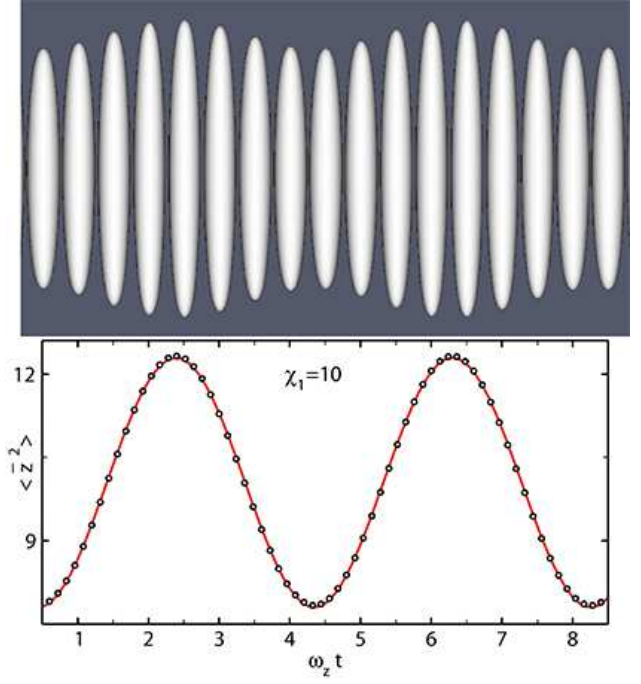


FIG. 4: Evolution of a ^{87}Rb condensate with $\chi_1 = 10$ and no vortices, in a trap with $\lambda = 0.1$ after a 10% fluctuation in the axial trap frequency. Top: isosurfaces of the condensate density taken at intervals $\Delta t = 0.5\omega_z^{-1}$. Bottom: evolution of the mean squared axial amplitude ($\bar{z} \equiv z/a_z$). Open circles correspond to the numerical data and the solid line is the best sinusoidal fit to these data.

magnetic trap with axial frequency $\omega_z = 2\pi \times 3$ Hz and different radial frequencies $\omega_\perp = \omega_z/\lambda$ with $\lambda \leq 1/10$. These condensates have a scattering length $a = 5.29$ nm and an oscillator length $a_z = 6.23$ μm . For condensates with a given vortex charge q , we vary the relevant parameter $\chi_1 = \sqrt{\lambda}Na/a_z$ by modifying the trap aspect ratio λ and/or the number of atoms N . For a given value of χ_1 we always start with $\lambda = 1/10$ and calculate the condensate equilibrium configuration in the trap. We then excite the axial breathing mode by introducing a small fluctuation in the axial frequency for a period of time $t = \omega_z^{-1}$ and let the condensate oscillate in the trap. At this stage we monitor the mean squared axial amplitude as a function of time and extract the corresponding oscillation frequency from a nonlinear least-squares fit of a sinusoidal function to the numerical data. We have considered different perturbations of the trap frequency, ranging from 1% to 10%, and different fitting intervals and have always obtained the same results within our required precision (better than 0.1%). Figure 4 displays an example corresponding to a condensate with 37220 atoms ($\chi_1 = 10$) and no vortices, in a trap with an aspect ratio $\lambda = 1/10$. The top panel shows the condensate evolution after a 10% perturbation in the axial trap frequency. The images are isosurfaces of the conden-

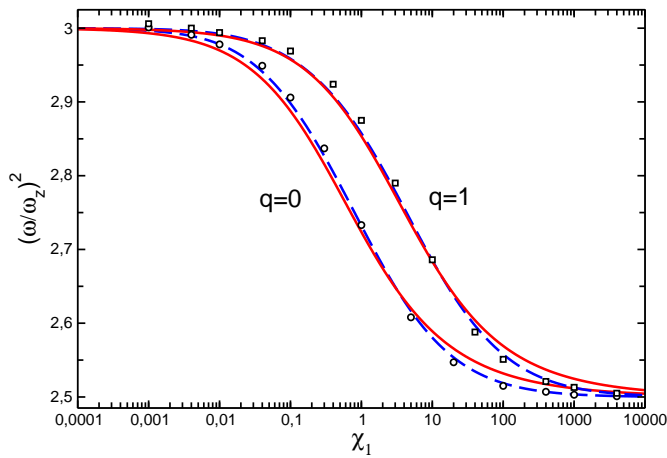


FIG. 5: Squared frequency of the axial breathing mode $(\omega/\omega_z)^2$ of highly elongated condensates with $q = 0$ and 1 , as a function of χ_1 . Open symbols are numerical results obtained from the full 3D GPE. Solid curves are the theoretical prediction from Eq. (53) and dashed curves are the theoretical prediction from Eq. (59).

satte density (corresponding to 5% of the maximum density) taken at intervals $\Delta t = 0.5\omega_z^{-1}$. The bottom panel shows the evolution of the mean squared axial amplitude in units of a_z^2 (\bar{z} stands for z/a_z). Open circles correspond to the numerical data and the solid line is the best sinusoidal fit to these data. From this fit we obtain an oscillation frequency $\omega = 1.605\omega_z$ with an accuracy better than 0.1%.

In general, a non-negligible contribution of the quantum pressure manifests itself as an appreciable dependence of the oscillation frequency on the parameter λ . For a given value of χ_1 , as λ increases the contribution of the quantum pressure also increases, producing in turn an increase in the condensate oscillation frequency. This fact can be used in particular to quantify the contribution of the quantum pressure or, equivalently, the validity of the local density approximation. To guarantee that the numerical results obtained are comparable with the above analytic formulas we have repeated the procedure explained before using smaller and smaller values of λ until reaching an oscillation frequency exhibiting no appreciable dependence on λ . An estimation of the values required can be obtained from Eq. (40). Figure 5 shows the (squared) frequency of the axial breathing mode $(\omega/\omega_z)^2$ of highly elongated condensates with vorticity $q = 0$ and 1 , as a function of χ_1 . Open symbols are numerical results obtained from the full 3D GPE with an accuracy of the order of 0.1%. Solid curves are the theoretical prediction from Eqs. (53) and (25) and dashed curves are the theoretical prediction from Eqs. (59) and (25). Equation (53) reproduces the numerical results with an accuracy better than 0.8% for $q = 0$ and better than 0.9% for $q = 1$. Equation (59) is somewhat more accurate. It reproduces the numerical results with an accuracy better than 0.4% for $q = 0$ and better than 0.65%

for $q = 1$. As Fig. 5 reflects, in the crossover between the TF and the quasi-1D mean-field regimes there exists a clear dependence of the frequency ω on the vortex charge q . This fact could be used for an indirect detection of unit-charge vortices in the crossover regime. Because of their accuracy and range of applicability the above formulas could also be useful from an experimental point of view, for instance, for calibration of the trap frequencies.

V. CONCLUSION

In this work, by using the adiabatic approximation in combination with a variational approach for determining the local chemical potential associated with the corresponding radial equation, we have derived different effective 1D equations of motion for the axial dynamics of highly elongated condensates. We have shown that the minimization of the radial energy functional within a subspace of convenient variational trial functions leads to the NPSE. We also have demonstrated that in certain cases a variational approach based on the chemical-potential functional can produce better results than the usual variational approach based on the energy functional. In this regard, while the minimization of the energy functional within the whole space of admissible functions always yields the correct chemical potential, the same does not remain true when this minimization is restricted to a certain variational subspace. In fact, we have seen that in this case it is possible to obtain a more simple and yet more accurate result by minimizing directly the chemical-potential functional. By doing this, we have derived a new effective 1D equation of motion which, for condensates with vorticity $|q| = 0$ and 1 , coincides exactly with our previous proposal, obtained in Ref. [28] by using a suited TF-like ansatz. The variational approach followed in this work provides us with a unified method for obtaining the different effective 1D equations in a systematic way and permits us to appreciate clearly the differences and similarities between the various proposals. A direct comparison with numerical results from the full 3D GPE indicates that the effective 1D equation proposed in Ref. [28] is the one that gives a more accurate description of the condensate axial dynamics. This equation also has the advantage that, in combination with the local density approximation, it allows to derive accurate analytical formulas for a number of ground-state properties. These formulas are valid and accurate (with an accuracy typically better than 1%) not only in the TF and in the quasi-1D mean-field regime, but also in between these two limiting cases. Moreover, since they only depend on an easily measurable physical quantity (the condensate axial half-length) they can be useful for a more precise experimental characterization of these kind of systems.

We also have obtained an expression for the axial healing length of elongated condensates and have found that, in the local density approximation and in units of the axial

oscillator length, it coincides with the inverse of the condensate axial half-length. From this result it immediately follows the necessary condition for the validity of the local density approximation.

Finally, we have obtained approximate analytic formulas that give the frequency of the axial breathing mode of an elongated condensate with accuracy better than 1% and remain valid in the crossover between the TF and the quasi-1D mean-field regimes. These formulas, which as the rest of the ground-state properties can be expressed in terms only of the axial half-length Z , could be relevant from an experimental point of view since in the crossover regime (the regime where most experiments are carried out) the usual formulas are not applicable.

This work has been supported by MEC (Spain) and FEDER fund (EU) (Contract No. Fis2005-02886).

* Electronic address: ammateo@ull.es

† Electronic address: vdelgado@ull.es

- [1] M. Olshanii, Phys. Rev. Lett. **81**, 938 (1998).
 [2] D. S. Petrov, G. V. Shlyapnikov, and J. T. M. Walraven, Phys. Rev. Lett. **85**, 3745 (2000).
 [3] V. Dunjko, V. Lorent, and M. Olshanii, Phys. Rev. Lett. **86**, 5413 (2001).
 [4] K. K. Das, Phys. Rev. A **66**, 053612 (2002).
 [5] A. Görlitz, J. M. Vogels, A. E. Leanhardt, C. Raman, T. L. Gustavson, J. R. Abo-Shaer, A. P. Chikkatur, S. Gupta, S. Inouye, T. Rosenband, and W. Ketterle, Phys. Rev. Lett. **87**, 130402 (2001).
 [6] C. Menotti and S. Stringari, Phys. Rev. A **66**, 043610 (2002).
 [7] W. Guerin, J.-F. Riou, J. P. Gaebler, V. Josse, P. Bouyer, and A. Aspect, Phys. Rev. Lett. **97**, 200402 (2006).
 [8] A. I. Nicolin, R. Carretero-González, and P. G. Kevrekidis, Phys. Rev. A **76**, 063609 (2007).
 [9] R. Carretero-González, D. J. Frantzeskakis and P. G. Kevrekidis, Nonlinearity **21**, R139 (2008).
 [10] W. Hansel, P. Hommelhoff, T.W. Hansch, and J. Reichel, Nature **413**, 498 (2001).
 [11] H. Ott, J. Fortagh, G. Schlotterbeck, A. Grossmann, and C. Zimmermann, Phys. Rev. Lett. **87**, 230401 (2001).
 [12] A. E. Leanhardt, A. P. Chikkatur, D. Kielpinski, Y. Shin, T. L. Gustavson, W. Ketterle, and D. E. Pritchard, Phys. Rev. Lett. **89**, 040401 (2002).
 [13] M. Greiner, I. Bloch, O. Mandel, T. W. Hänsch, and T. Esslinger, Phys. Rev. Lett. **87**, 160405 (2001).
 [14] H. Moritz, T. Stöferle, M. Köhl, and T. Esslinger, Phys. Rev. Lett. **91**, 250402 (2003).
 [15] S. Burger, K. Bongs, S. Dettmer, W. Ertmer, K. Sengstock, A. Sanpera, G. V. Shlyapnikov, and M. Lewenstein, Phys. Rev. Lett. **83**, 5198 (1999).
 [16] A. Weller, J. P. Ronzheimer, C. Gross, J. Esteve, M. K. Oberthaler, D. J. Frantzeskakis, G. Theocharis, and P. G. Kevrekidis, Phys. Rev. Lett. **101**, 130401 (2008).
 [17] Y. Shin, M. Saba, T. A. Pasquini, W. Ketterle, D. E. Pritchard, and A. E. Leanhardt, Phys. Rev. Lett. **92**, 050405 (2004).
 [18] T. Schumm, S. Hofferberth, L. M. Andersson, S. Wildermuth, S. Groth, I. Bar-Joseph, J. Schmiedmayer and P. Krüger, Nat. Phys. **1**, 57 (2005).
 [19] Y.-J. Wang, D. Z. Anderson, V. M. Bright, E. A. Cornell, Q. Diot, T. Kishimoto, M. Prentiss, R. A. Saravanan, S. R. Segal, and S. Wu, Phys. Rev. Lett. **94**, 090405 (2005).
 [20] E. P. Gross, Nuovo Cimento **20**, 454 (1961); J. Math. Phys. **4**, 195 (1963); L. P. Pitaevskii, Zh. Eksp. Teor. Fiz. **40**, 646 (1961) [Sov. Phys. JETP **13**, 451 (1961)].
 [21] A. D. Jackson, G. M. Kavoulakis, and C. J. Pethick, Phys. Rev. A **58**, 2417 (1998).
 [22] M. L. Chiofalo and M. P. Tosi, Phys. Lett. A **268**, 406 (2000).
 [23] L. Salasnich, A. Parola, and L. Reatto, Phys. Rev. A **65**, 043614 (2002).
 [24] P. Massignan and M. Modugno, Phys. Rev. A **67**, 023614 (2003).
 [25] A. M. Kamchatnov and V. S. Shchesnovich, Phys. Rev. A **70**, 023604 (2004).
 [26] W. Zhang and L. You, Phys. Rev. A **71**, 025603 (2005).
 [27] A. Muñoz Mateo and V. Delgado, Phys. Rev. A **75**, 063610 (2007); Phys. Rev. A **74**, 065602 (2006).
 [28] A. Muñoz Mateo and V. Delgado, Phys. Rev. A **77**, 013617 (2008);
 [29] Y. Shin, M. Saba, M. Vengalattore, T. A. Pasquini, C. Sanner, A. E. Leanhardt, M. Prentiss, D. E. Pritchard, and W. Ketterle, Phys. Rev. Lett. **93**, 160406 (2004).
 [30] A. Muñoz Mateo and V. Delgado, Phys. Rev. Lett. **97**, 180409 (2006).
 [31] J. A. Huhtamäki, M. Möttönen, T. Isoshima, V. Pietilä, and S. M. Virtanen, Phys. Rev. Lett. **97**, 110406 (2006).
 [32] H. M. Nilsen and E. Lundh, Phys. Rev. A **77**, 013604 (2008).
 [33] M. Krämer, C. Menotti and M. Modugno, J. Low Temp. Phys. **138**, 729 (2005).
 [34] G. Baym and C. J. Pethick, Phys. Rev. Lett. **76**, 6 (1996).
 [35] V. M. Pérez-García, H. Michinel, J. I. Cirac, M. Lewenstein, and P. Zoller, Phys. Rev. A **56**, 1424 (1997).
 [36] L. Salasnich, B. A. Malomed, and F. Toigo, Phys. Rev. A **76**, 063614 (2007).
 [37] S. Stringari, Phys. Rev. Lett. **77**, 2360 (1996).
 [38] Yu. Kagan, E. L. Surkov, and G. V. Shlyapnikov, Phys. Rev. A **54**, R1753 (1996).
 [39] Y. Castin and R. Dum, Phys. Rev. Lett. **77**, 5315 (1996).
 [40] A. Csordas and R. Graham, Phys. Rev. A **59**, 1477 (1999).
 [41] S. Stringari, Phys. Rev. A **58**, 2385 (1998).
 [42] T.-L. Ho and M. Ma, J. Low Temp. Phys. **115**, 61 (1999).